I would like to thank my parents Dr Gabriele and Dr Herwig Happe

For Marlene and Paula

This book was originally published in German under the title *Erfolg mit Implantaten in der ästhetischen Zone: Parodontale, implantologische und restaurative Behandlungsstrategien* in 2018 by Quintessenz Verlags-GmbH, Berlin, Germany.

Library of Congress Cataloging-in-Publication Data

Names: Happe, Arndt, editor. | Körner, Gerd, editor.
Title: Techniques for success with implants in the esthetic zone / edited by Arndt Happe and Gerd Körner.
Other titles: Erfolg mit Implantaten in der ästhetischen Zone. English.
Description: Batavia, IL : Quintessence Publishing Co, Inc, [2019] | Includes bibliographical references and index.
Identifiers: LCCN 2019019189 | ISBN 9780867158229 (hardcover)
Subjects: | MESH: Dental Implantation | Esthetics, Dental
Classification: LCC RK667.I45 | NLM WU 640 | DDC 617.6/93--dc23
LC record available at https://lccn.loc.gov/2019019189

QUINTESSENCE PUBLISHING USA

Quintessence Publishing Co, Inc
411 N Raddant Road
Batavia, IL 60510
www.quintpub.com

5 4 3 2 1

Editor: Marieke Zaffron
Design: Sue Zubek
Production: Kaye Clemens and Christine Cianciosi

Printed in China

Contents

Contributors

Christian Coachman, DDS, CDT
Founder
Digital Smile Design
São Paulo, Brazil

Vincent Fehmer, MDT
Division of Fixed Prosthodontics and Biomaterials
Clinic of Dental Medicine
University of Geneva
Geneva, Switzerland

Pascal Holthaus, ZTM
Master Dental Technologist
Münster, Germany

Tomohiro Ishikawa, DDS
Private Practice
Hamamatsu, Japan

Tal Morr, DMD, MSD
Private Practice Limited to Prosthodontics
Miami, Florida

Daniel Rothamel, MD, DMD, PhD
Professor
Department of Maxillofacial and Plastic Surgery
University Hospital of Düsseldorf
Düsseldorf, Germany

Head of the Division of Maxillofacial Surgery
Protestant Hospital Bethesda
Mönchengladbach, Germany

Irena Sailer, Prof Dr Med Dent
Head
Division of Fixed Prosthodontics and Biomaterials
Clinic of Dental Medicine
University of Geneva
Geneva, Switzerland

Anja Zembic, PD, DMD
Consultant
Department of Fixed and Removable Prosthodontics
University of Zürich
Zürich, Switzerland

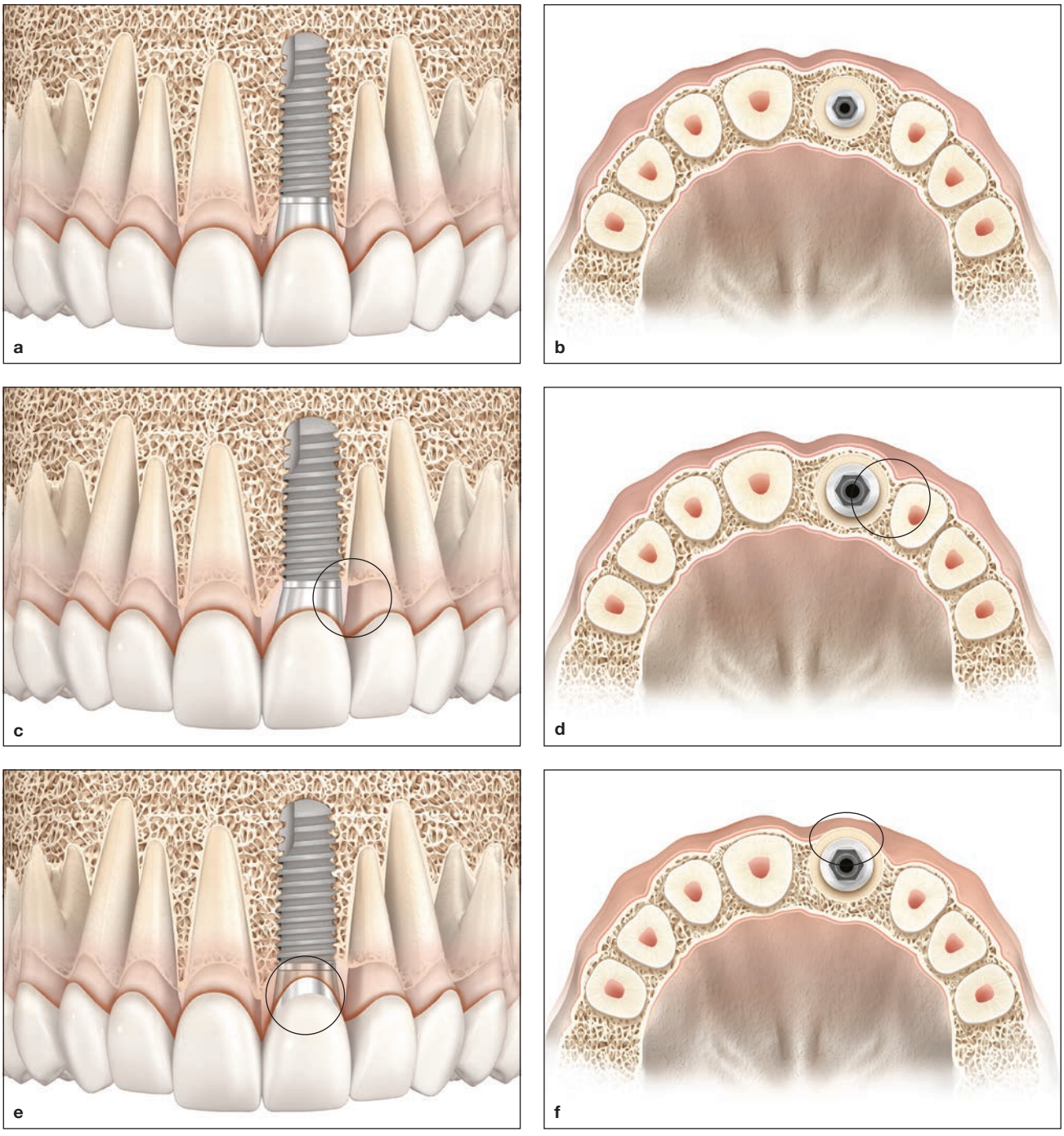

Fig 1-6 / *(a and b)* Anatomy around non-platform-switched implants. *(c and d)* Excessively large diameter and malpositioning distally lead to loss of papilla. *(e and f)* Excessively large diameter and malpositioning buccally lead to recession.

latter effect usually does not occur with single-tooth implants because the attachment of adjacent teeth determines papilla height. However, it is a major problem with adjacent implants and makes the reconstruction of papillae between adjacent implants highly unpredictable (Figs 1-6g to 1-6j and Fig 1-7).[26] These circumstances and their influence on esthetics were described graphically by Grunder et al[26] as early as 2005 and motivated the use of platform switching to exert a positive effect on the peri-implant bone situation. As a result, components reduced in diameter came to be used to move the microgap away from the bone in a central direction (see Fig 1-5b).

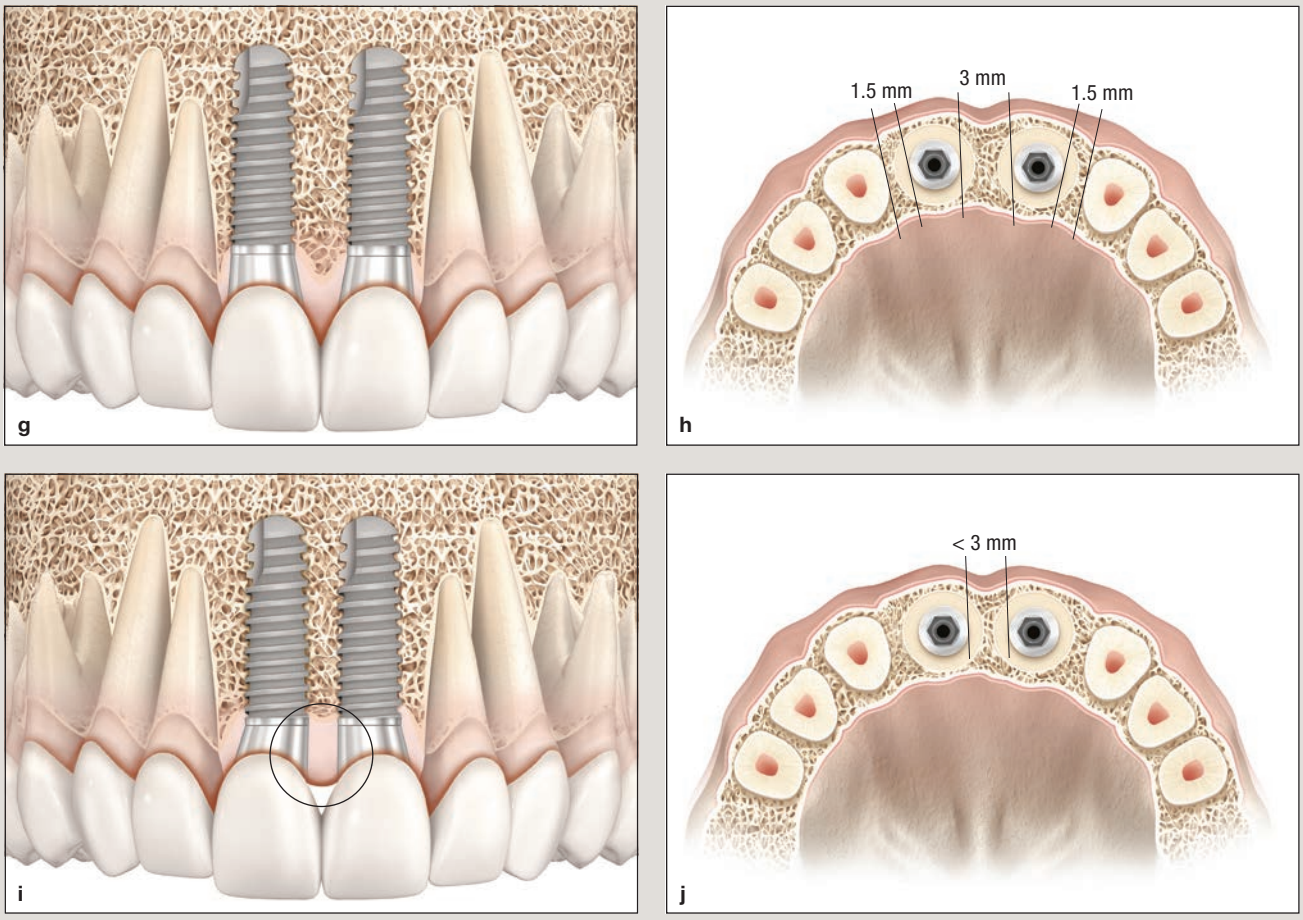

Fig 1-6 *cont.* / *(g and h)* Recommended distances for adjacent implants. *(i and j)* Adjacent implants placed too close together lead to loss of papilla. (Adapted with permission from Grunder et al.[26])

Fig 1-7 / *(a)* Implant design with smooth (ie, machined) 1.4-mm shoulder. *(b)* All-ceramic restorations after full-mouth reconstruction, including implants placed at the maxillary right lateral incisor and canine sites and the mandibular right canine site. The interproximal soft tissue between the maxillary lateral incisor and canine is deficient. (Laboratory work performed by A. Nolte.)

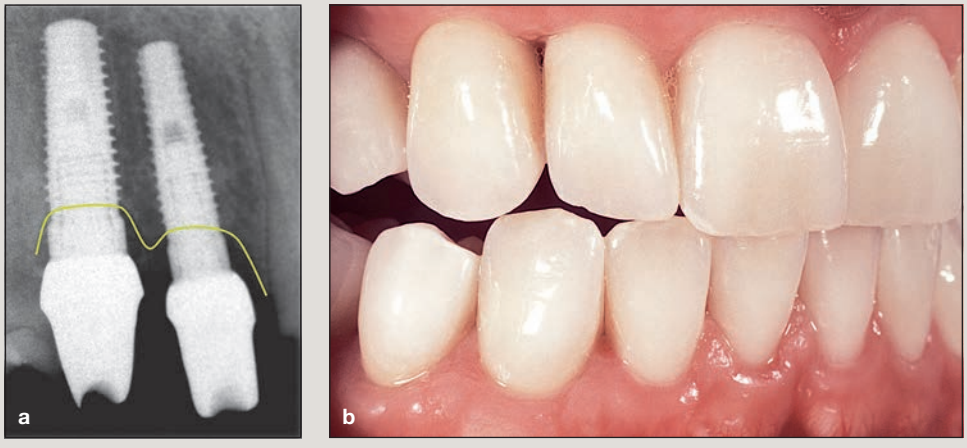

Fig 3-2 / Microsurgery instrument tray.

Fig 3-3 / Microsurgical needle holder, forceps, and scissors.

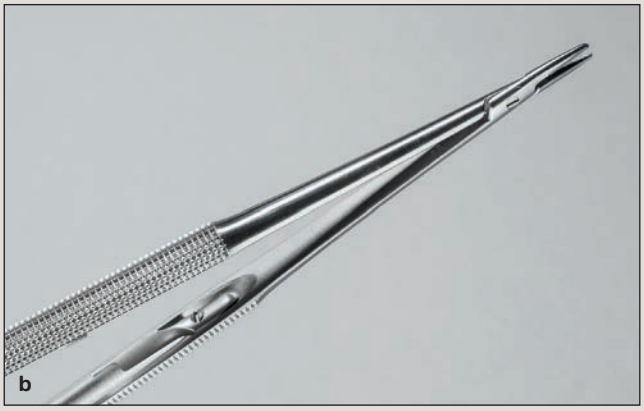

Fig 3-4 / *(a and b)* Examples of straight microneedle holders.

Fig 3-5 / *(a and b)* Examples of microsuture scissors.

Fig 4-8 *cont.* / *(q to s)* Clinical photographs 5 years after treatment. *(t)* Final portrait. (Surgery and prosthodontics performed by A. Happe; laboratory work performed by P. Holthaus.)

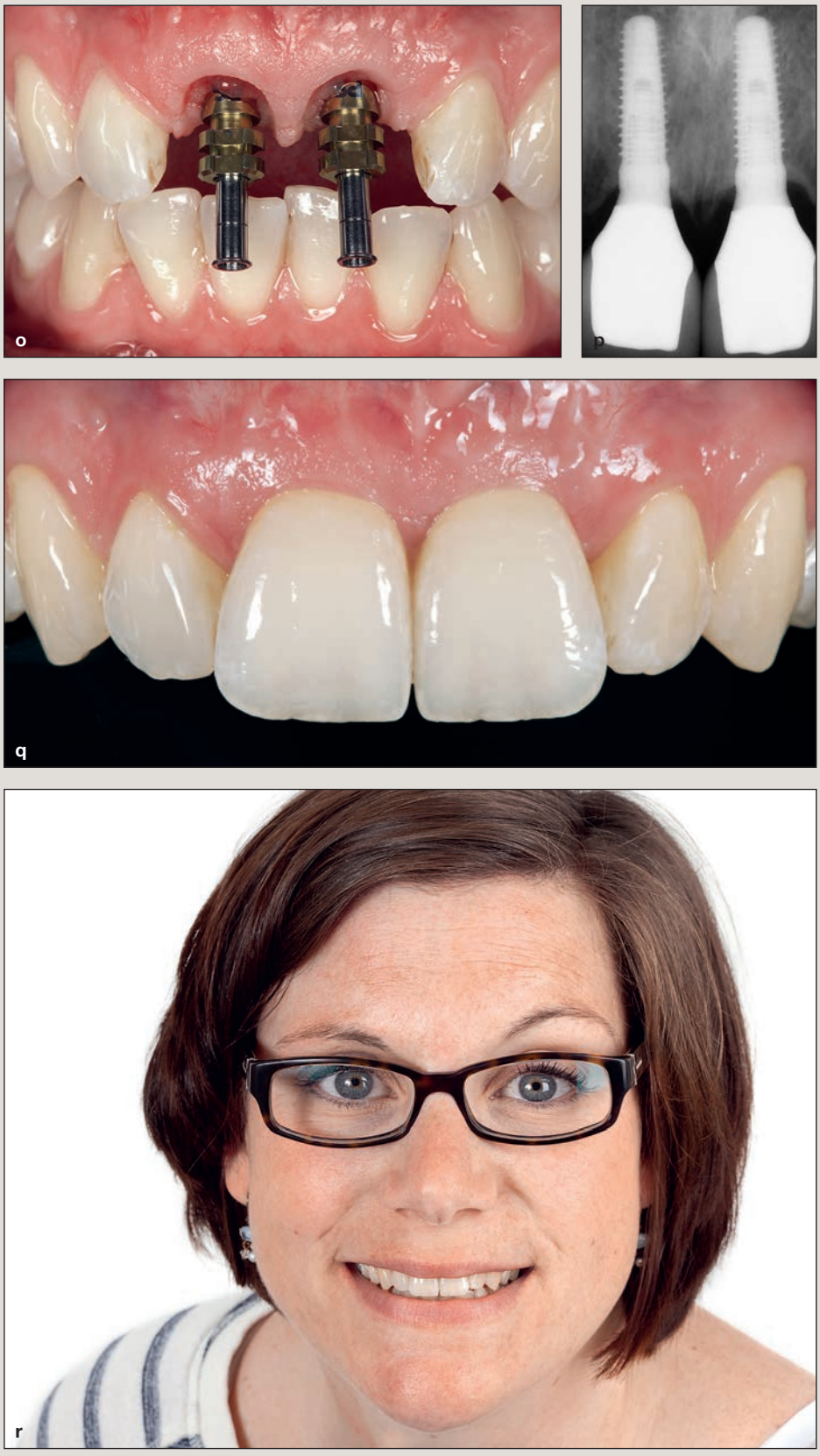

Fig 4-9 *cont.* / *(o)* Taking impressions of the implants. *(p)* Radiograph of the superstructure 1 year after implant placement. Note the height of the interimplant bone, which is very important for supporting the papillae. *(q)* All-ceramic crowns 1 year after implant placement. *(r)* Portrait after completion of the treatment. (Surgery performed by A. Happe; prosthodontics performed by B. van den Bosch; laboratory work performed by A. Nolte.)

Fig 5-10 / 30-year-old patient. *(a)* Portrait before treatment. *(b)* Smile. *(c)* The maxillary right central incisor is fractured. The root remnant has a longitudinal fracture and is not worth preserving. *(d)* Protrusion. Discernible loss of substance at the incisal edges of the anterior teeth. *(e)* Occlusal view of the maxilla. There is moderate generalized erosion and partially inadequate restorations. *(f)* Occlusal view of the mandible. There is moderate generalized erosion and partially inadequate restorations. *(g)* Radiograph superimposed over the clinical situation. *(h)* It must be decided how deep to place the implant.

Fig 5-11 *cont.* / *(j)* Esthetic analysis: The horizontal and vertical reference planes and smile line were transferred to the portrait. *(k)* Magnification of the mouth area. *(l)* The key reference planes were transferred to the intraoral situation. *(m)* The digital ruler is calibrated to the real crown length of the right central incisor. *(n)* Once calibrated, the ruler can be used for approximate measurement of dimensions on the image. *(o)* The mucosa was depicted in black and white so that the tooth shapes could be assessed more efficiently. *(p)* The teeth were depicted in black and white to help assess the soft tissue contour. *(q)* Visualization of the width-to-length ratios of the right central incisor and left lateral incisor.

Fig 5-11 *cont.* / *(oo)* Frontal view of the definitive restoration. *(pp and qq)* Lateral views of the definitive restoration. *(rr)* Final portrait.

Fig 5-13 *cont.* / *(q and r)* Intraoral situation from left and right after completion of treatment. *(s and t)* Lateral views of smile after completion of treatment. *(u)* Final portrait. (Surgery and prosthodontics performed by A. Happe; laboratory work performed by A. Kunz.)

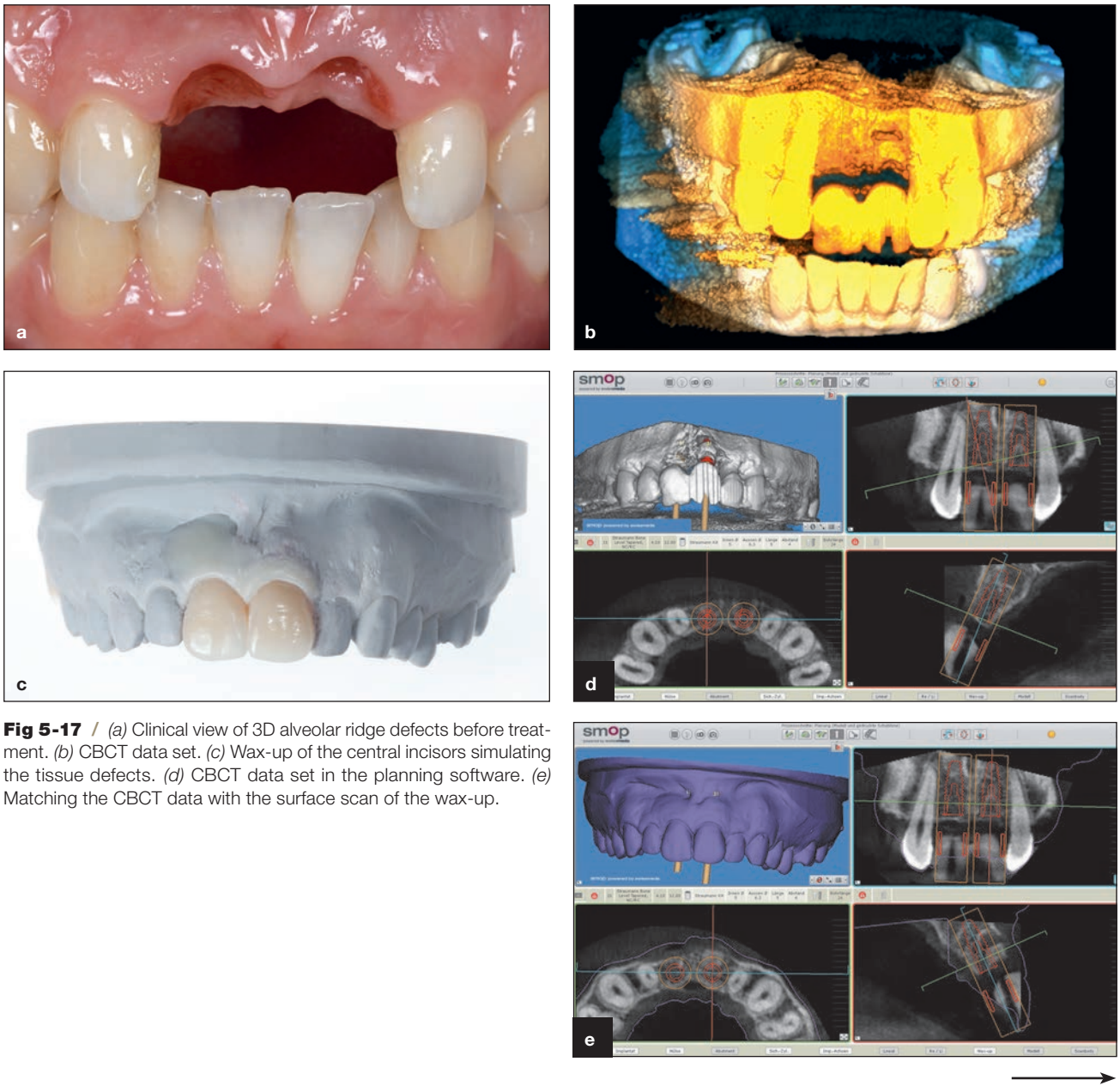

Fig 5-17 / *(a)* Clinical view of 3D alveolar ridge defects before treatment. *(b)* CBCT data set. *(c)* Wax-up of the central incisors simulating the tissue defects. *(d)* CBCT data set in the planning software. *(e)* Matching the CBCT data with the surface scan of the wax-up.

to independently upload the data sets and perform surgical planning with all of the prosthetic references. This approach allows for maximum freedom of software selection; the only requirement is that the system must be able to read the data in the standard STL format. These cloud-based systems also have the advantage of enabling different practitioners to work on a case simultaneously, thus greatly simplifying coordination with the referring clinician.

After all thorough examinations have been completed and the results and options discussed with the patient, the clinician can take a CBCT scan and upload the data into the planning software without any preliminary work by a dental technician (see Fig 5-17d). After an initial review of the findings, the clinician can share the planning data and discuss the case with colleagues and/or dental technicians via cloud-based technology. With the corresponding alginate impression or intraoral impression, the dental technician can then produce any type of setup or wax-up needed. This may require an intraoral try-in as an intermediate step, or it may be generated by the software directly as STL data via a scan. To start the matching process, the user must first upload and open the files containing the surface scan data of the current intraoral situation and the planning data for the future restoration (wax-up or setup) (see Fig 5-17e). As with the

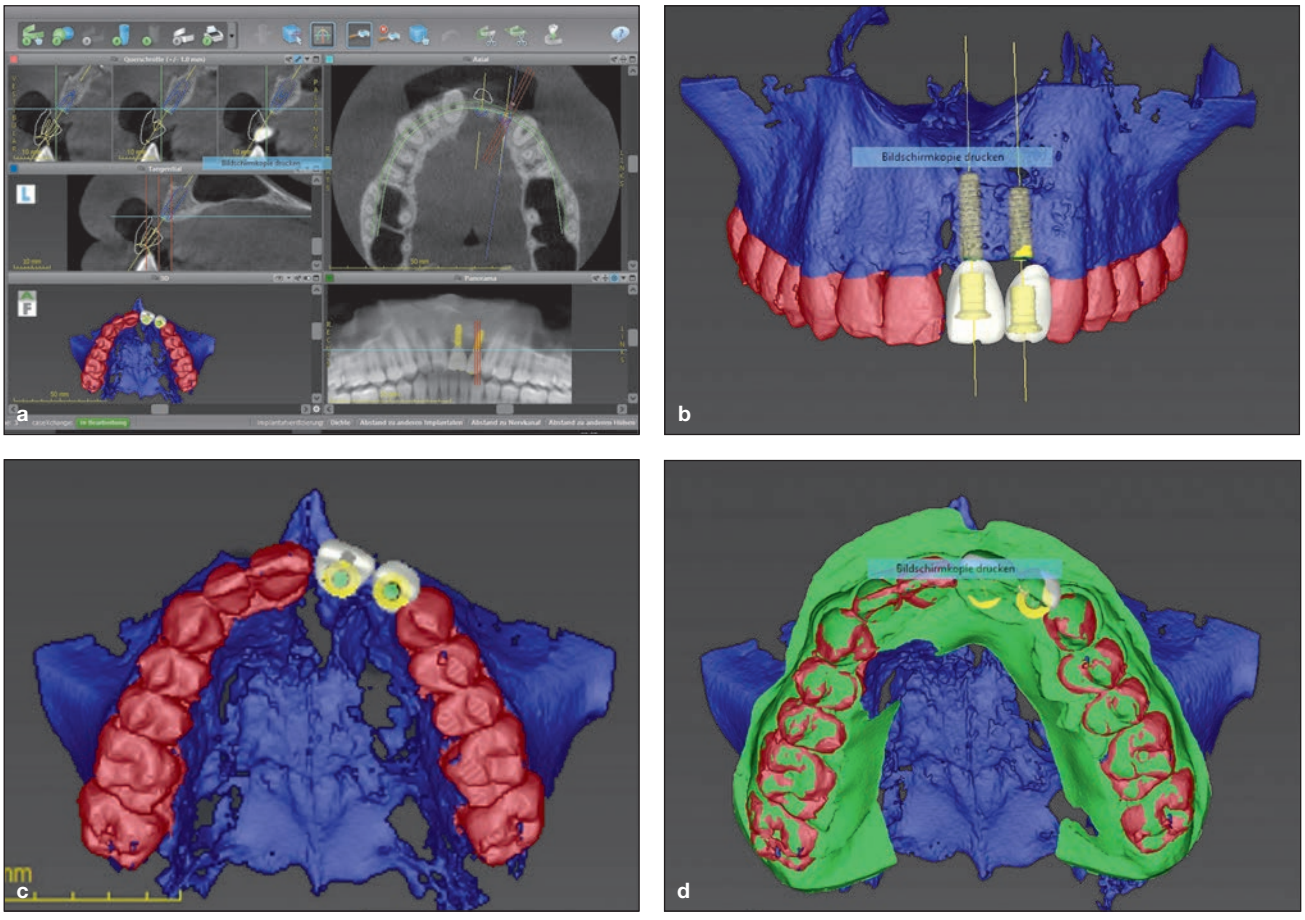

Fig 5-18 / *(a)* Overview of the different planning software views. *(b)* Digital wax-up of the maxillary left incisors. *(c)* Occlusal view of the digital wax-up: palatal screw retention is planned. *(d)* Surface scanned data matched with the CBCT data.

several versions of the surgical guide without reimporting the data, which means different treatment options can be presented to the team and the patient.[23] Once the final planning version of the surgical guide has been approved, the guide can be fabricated directly in the dental laboratory or ordered from the software manufacturer, if applicable (see Figs 5-17f and 5-17g). The splint module of the SMOP software package (SwissMeda) used to design the drill guide also produces STL data sets. Like all other systems currently available, this software contains details about all the relevant implant systems and the drill sleeves that accompany them. The SMOP workflow also has another interesting feature: Depending on which implant system is used, it may be possible to save the metal sleeve, which simplifies the manufacturing process and reduces costs, and also minimizes another source of error (eg, fitting the sleeves, luting the sleeves).[24,25] Unfortunately, this software only supports the implant-planning program and cannot be used in the restorative phase.

Creating a digital wax-up directly with the planning software

With this option, it is not only possible to upload and match the surface scan data of the current intraoral situation with the 3D CBCT data (as with the previously described options), but a digital wax-up can be created directly with the planning software (Figs 5-18a to 5-18d). Performing the workflow in this manner is highly efficient because the steps involved in displaying and then scaling and correctly positioning the virtual wax-up in the software can be completed very quickly.[26,27] Most guided surgery systems available today, however, are intended for planning purposes only. They are equipped with rather rudimentary tooth libraries and design software tools. These are sufficient for single-tooth implant planning if there are enough prosthetic references, including those on the adjacent teeth; however, if they are used for cantilever and partial denture restorations that span multiple teeth, proper adaptation and positioning of the

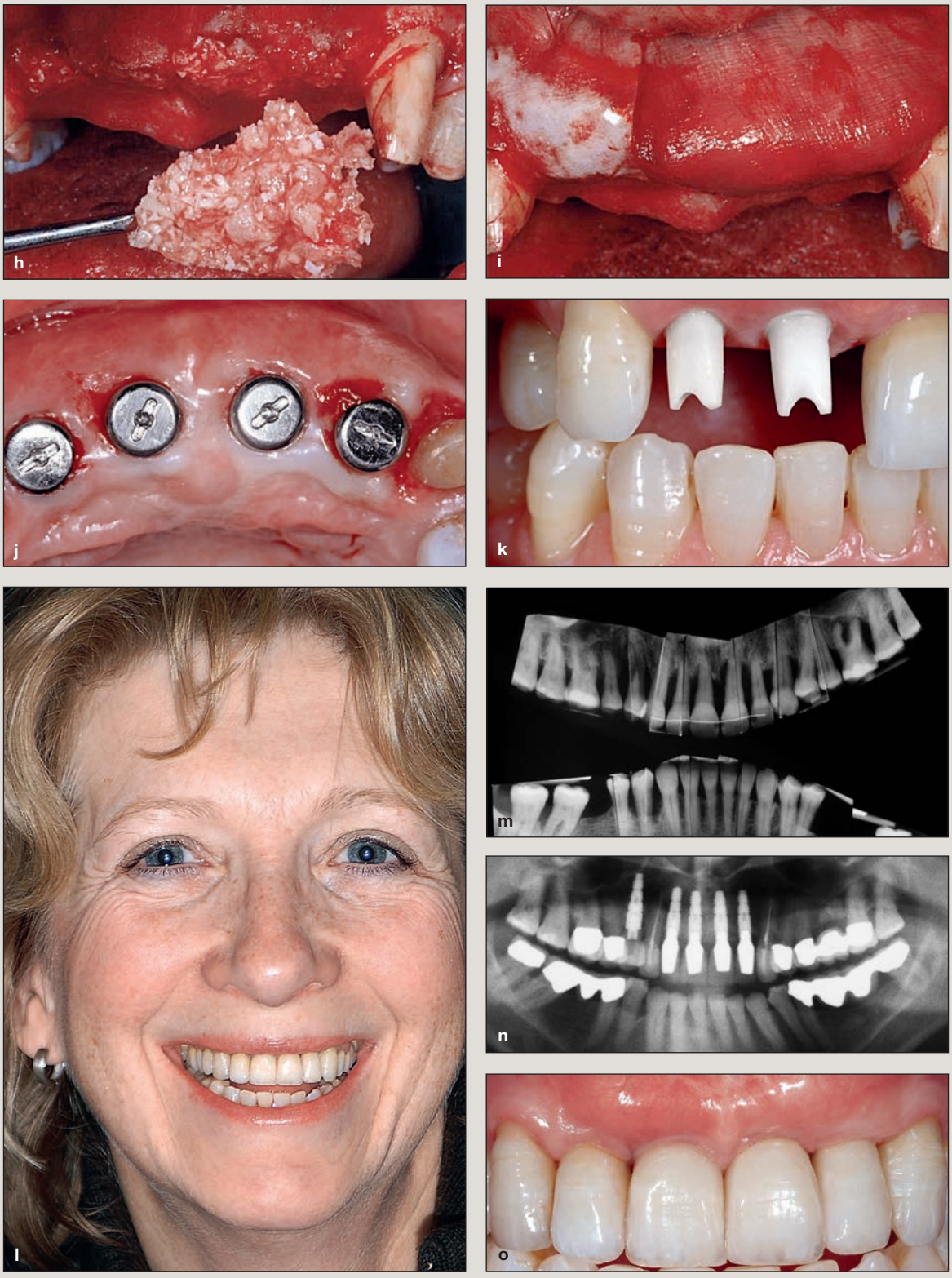

Fig 6-1 *cont.* / *(h)* Bone particulate augmentation in conjunction with plasma rich in growth factors (PRGF) for the horizontal deficits of the incisors. *(i)* Membrane coverage (Bio-Gide, Geistlich) of the mixed autogenous and xenogeneic augmentation material (Bio-Oss, Geistlich). *(j)* Minimally invasive exposure by the keyhole access expansion technique according to Happe et al.[4] *(k)* All-ceramic restorative treatment: implants with zirconia hybrid abutments at maxillary right first premolar and all maxillary incisors. *(l)* Final portrait after combined periodontal, implant, and restorative treatment. *(m)* Pretreatment radiograph. *(n)* Follow-up radiograph 6 years after completion of the treatment. The radiograph also shows socket preservation of the region of the maxillary left first molar and status after guided tissue regeneration (GTR) at the region of the mandibular right canine, first premolar, and second molar. *(o)* Clinical view of the maxillary anterior dentition 6 years after completion of the treatment. (Surgery and prosthodontics performed by G. Körner; laboratory work performed by K. Müterthies.)

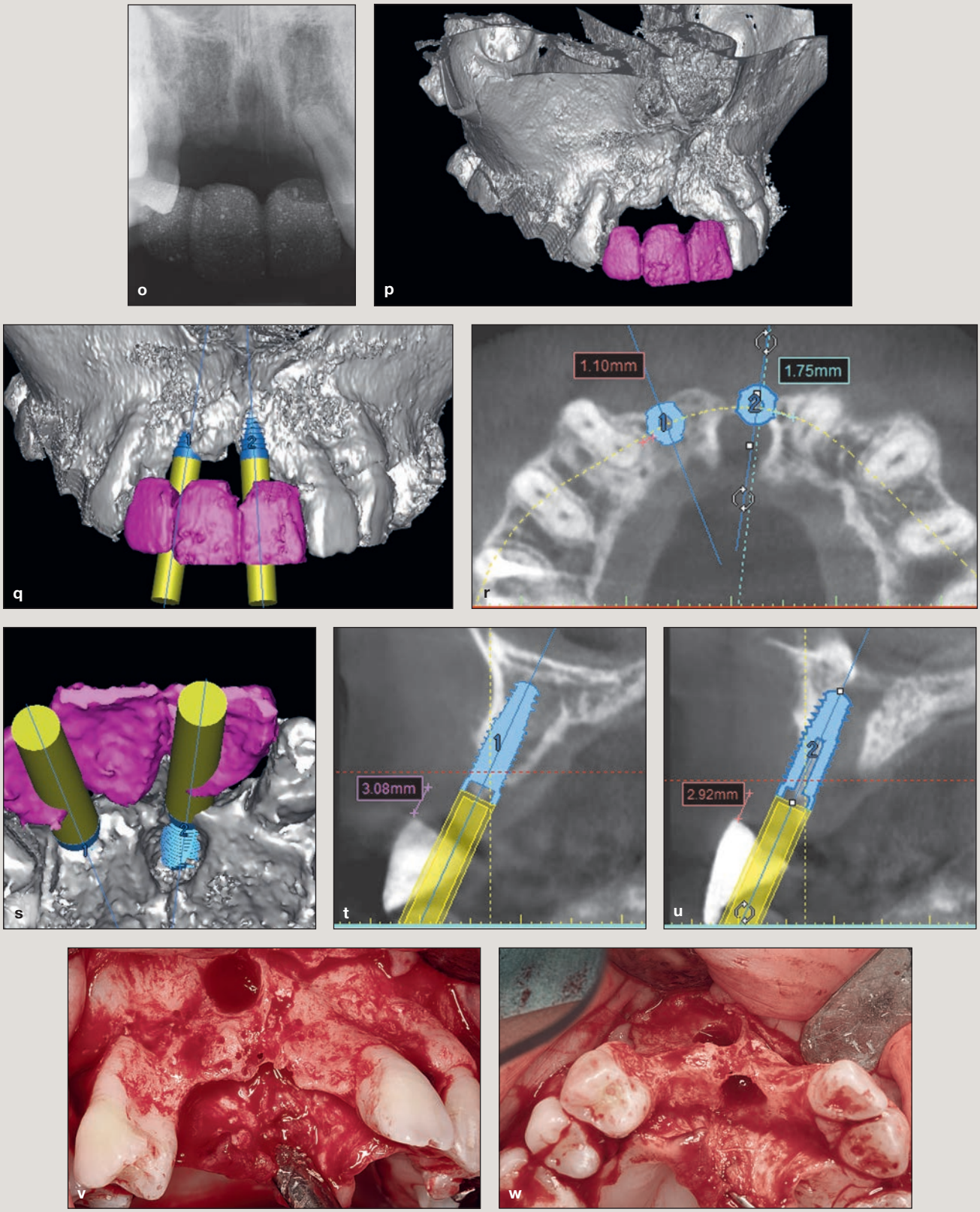

Fig 7-13 *cont.* / *(o to r)* Radiograph and CBCT scan before ridge reconstruction. The CBCT and radiograph with diagnostic template in place showed that the alveolar ridge had significant 3D hard and soft tissue defects. *(s to u)* The computer simulation prior to bone augmentation shows that the space for implant placement in the region of the right lateral incisor and left central incisor is inadequate. Furthermore, the angulation of the left lateral incisor and the prominent incisive canal prevent an ideal implant position. *(v and w)* The root eminences show the incorrect inclination of the teeth bordering the gap. The bone was cleaned of soft tissue, and the neurovascular bundle was removed from the incisive canal.

Fig 7-13 *cont.* / *(ddd to fff)* The end result. Although the patient presented with severe tissue damage, adequate tissue and papilla reconstruction was achieved, resulting in restored esthetics and function. *(ggg)* Photograph after 3 years of function showing soft tissue formation. *(hhh and iii)* Portrait after the treatment. Despite the high smile line, the patient is able to smile with confidence. (Orthodontics performed by K. Kida; laboratory work performed by M. Hinoshita.)

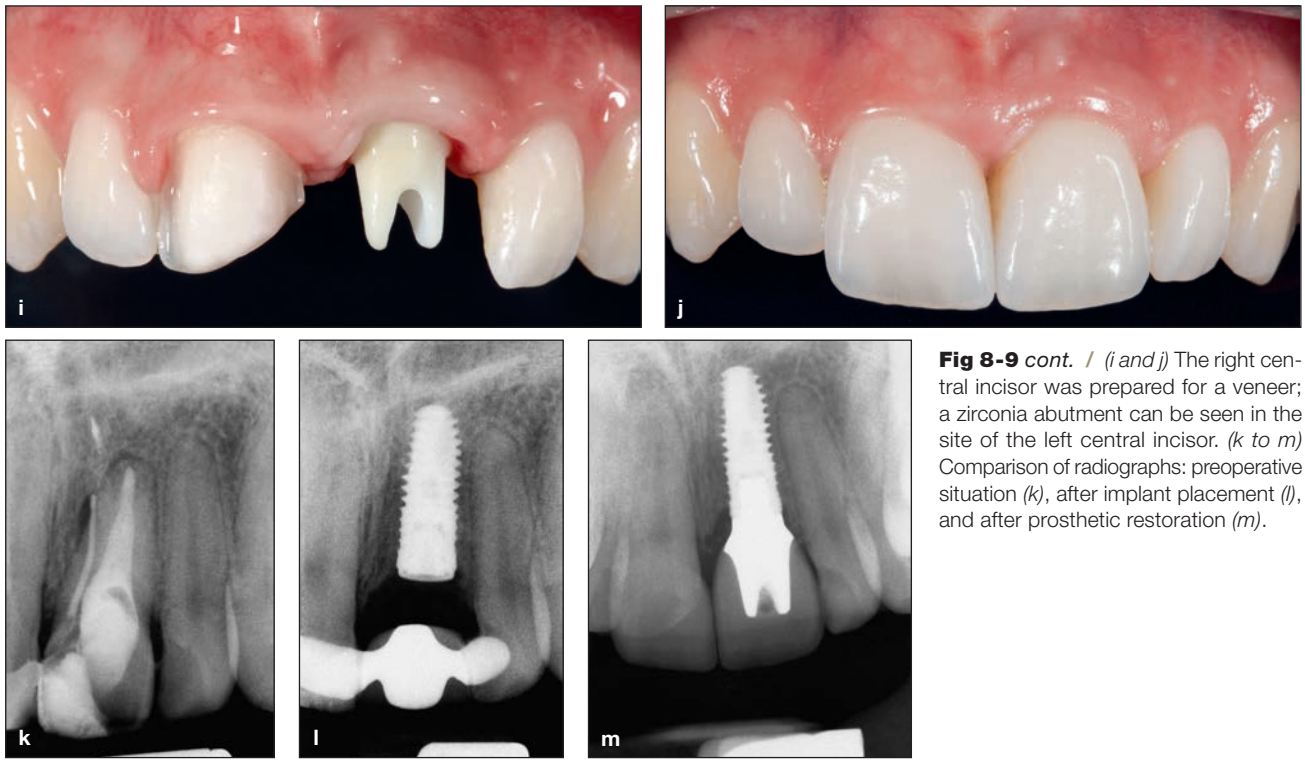

Fig 8-9 *cont.* / *(i and j)* The right central incisor was prepared for a veneer; a zirconia abutment can be seen in the site of the left central incisor. *(k to m)* Comparison of radiographs: preoperative situation *(k)*, after implant placement *(l)*, and after prosthetic restoration *(m)*.

Fig 8-9g). The horizontal contour of the alveolar process was anatomically correct after minimally invasive implant exposure as a result of soft tissue displacement and maturation (see Fig 8-9h). The dentofacial esthetics were restored with a veneer on the right central incisor and a zirconia abutment with an all-ceramic crown on the left central incisor implant (see Figs 8-9i and 8-9j). However, the case also shows collapse of the papillae mesial and distal to the implant.

The use of soft tissue grafts can often improve the clinical situation, especially where there are hard or soft tissue defects of variable severity that are already evident prior to extraction (see Figs 8-9k to 8-9m). As a result, the baseline situation for the subsequent procedure is greatly improved because resorptive defect healing is prevented. There is also an enhanced baseline situation for further surgical interventions.

Clinical case 2

A young patient presented with a fistula and horizontal root fracture in the middle third of the maxillary right central incisor (Fig 8-10). Both facially and palatally, it was possible to palpate down to the apex with the periodontal probe. Buccal and palatal lamellae had been lost. To achieve a favorable preoperative situation for augmentation and prevent collapse of the tissue, the socket was filled with collagen, and the entrance to the socket was sealed with a free punch graft. The graft needed to be at least 3 mm thick, and the soft tissue alveolar margins had to be trimmed with a rotary diamond or scalpel. After about 6 weeks, the tissue had healed and matured enough to allow for unproblematic flap formation. In this case, augmentation ensued with autogenous bone grafts (bone chips) and a laser-perforated titanium membrane (Frios Bone Shield, Dentsply).

Clinical case with subepithelial CTG

After an anterior tooth trauma with complete luxation (avulsion) and reimplantation of the two central incisors in his youth, the patient presented several years later with massive external resorption at the maxillary left central incisor (Fig 8-11). The buccal bone lamella together with mucosa was absent, which resulted in a hard and soft tissue defect. The lack of fixed keratinized mucosa, in particular, makes adequate soft tissue management difficult in augmentation surgery and might cause functional problems in the peri-implant area in the long term. Im-

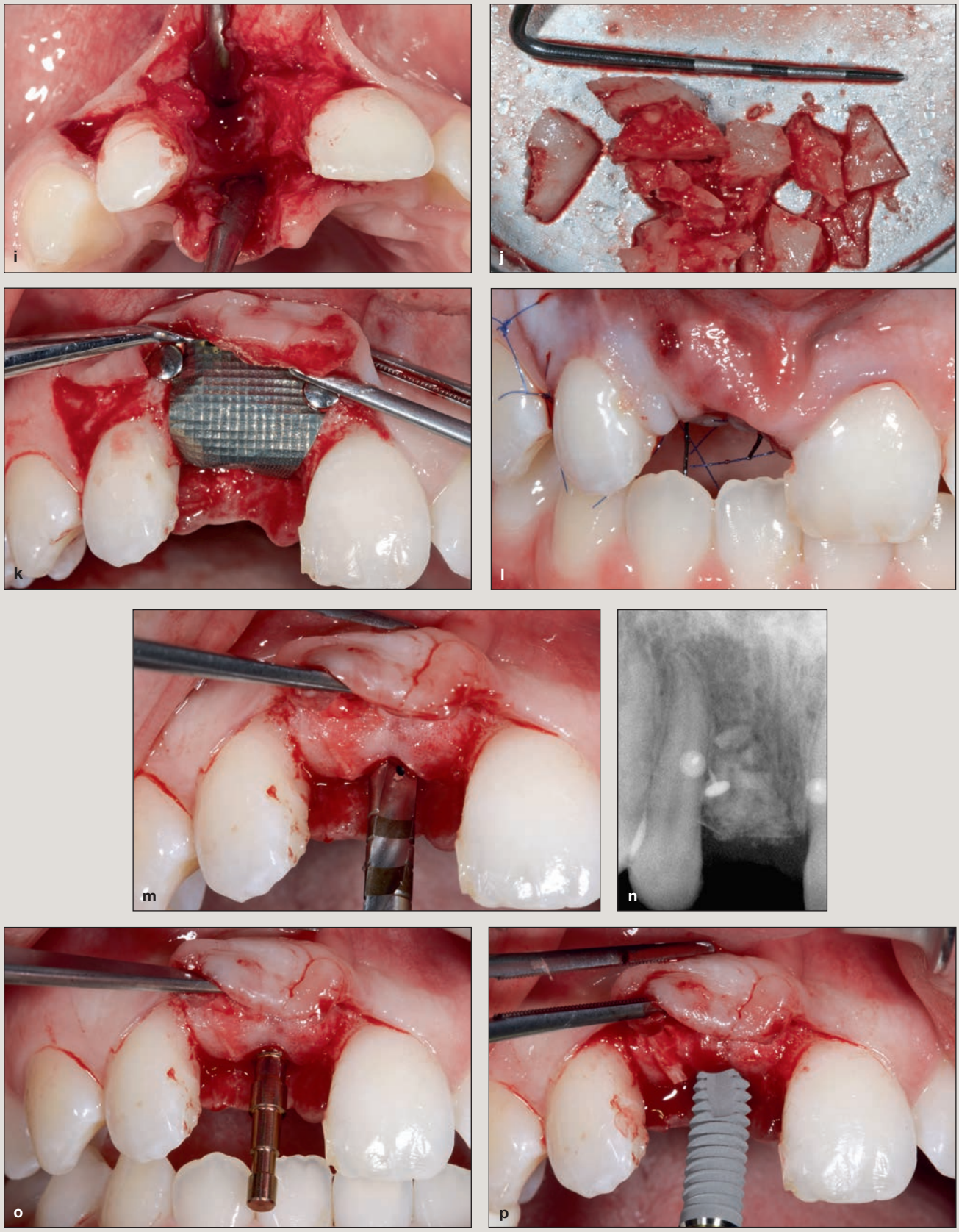

Fig 8-10 *cont.* / *(i)* Occlusal view of the defect. *(j)* Autogenous bone graft from the right retromolar region. *(k)* Augmented area with laser-perforated titanium membrane fixed with titanium pins. *(l)* Condition immediately after augmentation. Only one relieving incision was placed distal to the distal adjacent tooth. *(m)* After reopening and removal of the titanium membrane, regenerated alveolar ridge 3 months after augmentation can be observed. *(n)* Radiograph after augmentation. *(o)* Paralleling pin in place. *(p)* Placement of a 3.8-mm-diameter implant.

→

Fig 9-10 *cont.* / *(q and r)* Definitive restoration and smile after completion of treatment. *(s)* Pretreatment radiograph. *(t)* Radiograph of graft in place. *(u to x)* Radiographs after augmentation and at different stages of implant treatment. *(y)* Final portrait. (Surgery and prosthodontics performed by A. Happe; laboratory work performed by P. Holthaus.)

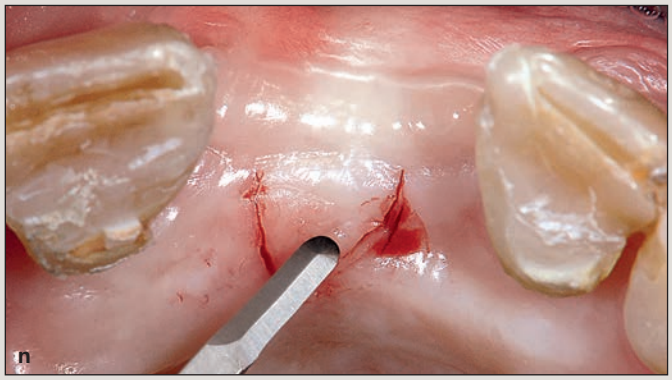

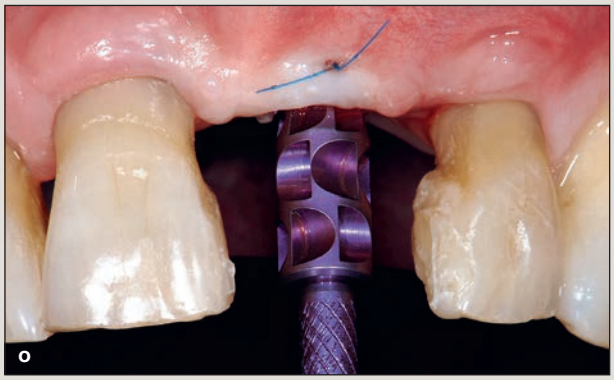

Fig 9-21 *cont.* / *(n)* Minimally invasive exposure with the roll flap technique. *(o)* The impression post is fitted during the prosthetic phase. *(p)* Intraoral view after the prosthodontic treatment with implant crown for the left central incisor and ceramic veneers on the adjacent teeth. *(q)* Portrait of the patient after treatment. (Surgery and prosthodontics performed by G. Körner; laboratory work performed by K. Müterthies.)

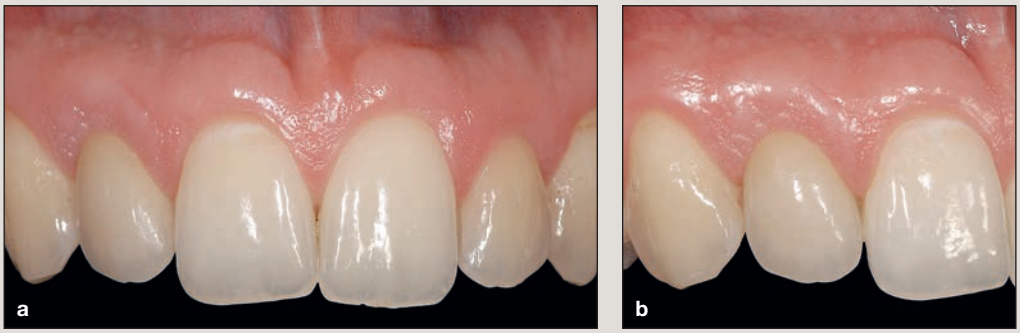

Fig 11-1 / *(a and b)* Five years after implant placement with a cement-retained all-ceramic crown on a zirconia abutment at the site of the right lateral incisor, the crown has a natural appearance with healthy and stable peri-implant mucosa.

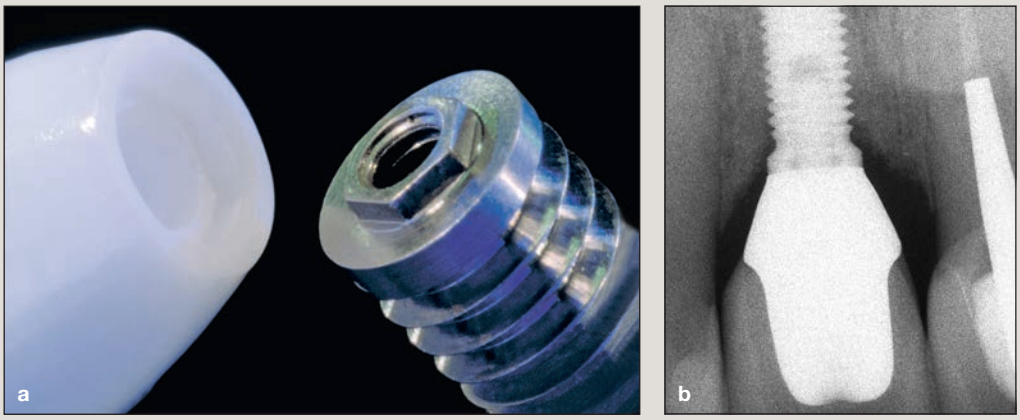

Fig 11-2 / *(a)* Externally connected zirconia abutment with butt joint and implant with external hex. (Courtesy of Dr Urs Brodbeck, Zürich, Switzerland.) *(b)* Radiograph of externally connected zirconia abutment with horizontal joining surfaces.

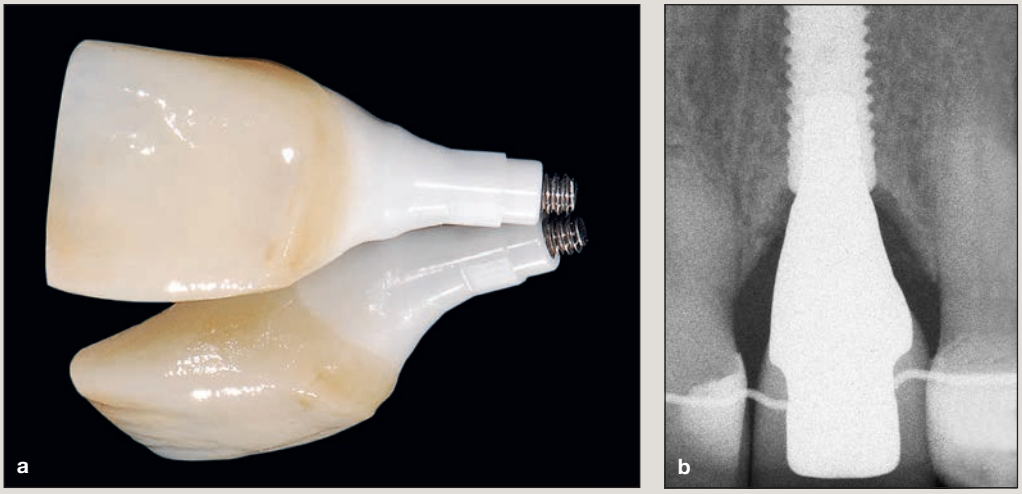

Fig 11-3 / *(a)* All-ceramic implant-supported crown cemented onto a single-piece zirconia abutment with an internal conical connection. *(b)* Radiograph of an internally connected zirconia abutment with a conical connection.

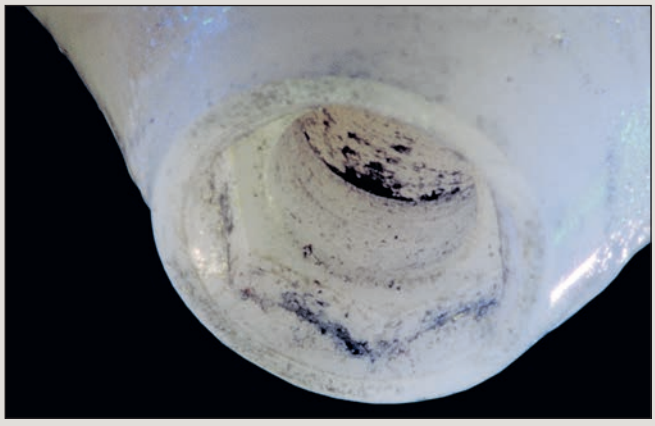

Fig 11-4 / Metallic particles demonstrating abrasive wear on the internal part of an externally connected zirconia abutment with a butt-joint connection. (Courtesy of Dr Urs Brodbeck, Zürich, Switzerland.)

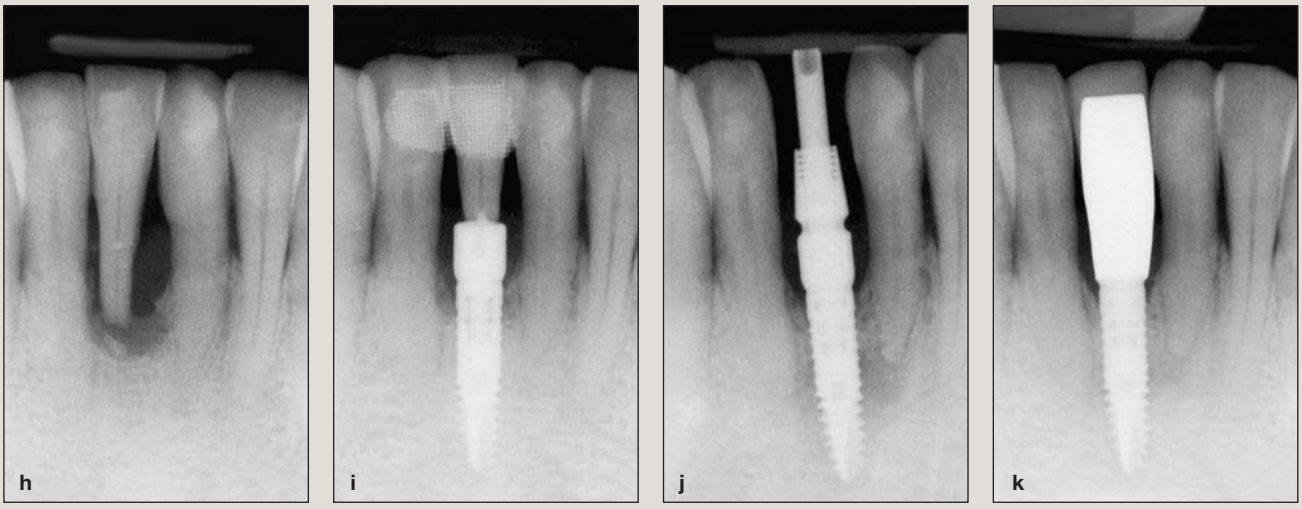

Fig 12-12 *cont.* / *(h to k)* Comparison of radiographs. *(h)* The radiograph shows that the mandibular right central incisor is not worth preserving. *(i)* Implant in situ. *(j)* Impression post in situ. *(k)* Completed superstructure in situ. (Surgery and prosthodontics performed by A. Happe; laboratory work performed by A. Nolte.)

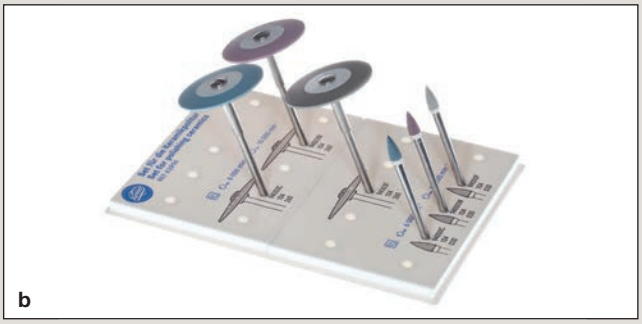

Fig 12-13 / *(a)* Polishing set for machining zirconia abutments. *(b)* Polishing set with rubber polishers for the handpiece. *(c and d)* All the subgingival areas of the abutment are only machined using the blue, red, and gray polishers and not brought to a high glaze with brushes and pastes. *(e)* Commercially available system for abutment cleaning (Finevo Reinigung, Sirius Ceramics).

Fig 13-9 *cont.* / *(i)* Smile after completion of the treatment. *(j)* Radiograph after augmentation. *(k)* Radiograph after implant placement. *(l)* Radiograph 6 months after completion of the prosthodontics. *(m)* Final portrait.

Failed augmentation attempts

Augmentation can fail for a variety of reasons. Aside from the previously mentioned soft tissue complications and resorptions caused by irritation or inflammation, the potential of bone substitute materials is often overestimated, or the indications for the material are not properly observed.[6] The limitations of the different techniques are described in chapter 9. The case illustrated in Fig 13-9 shows the condition after an unsuccessful augmentation attempt in the region of the maxillary right canine using bovine bone substitute and collagen membrane. However, because the buccal and palatal lamella were absent and this case involved a 3D ridge defect with a pronounced vertical component, the defect could only have been successfully treated with autogenous bone grafts. In this case, the defect was reconstructed with Khoury's bone plate technique.[7]

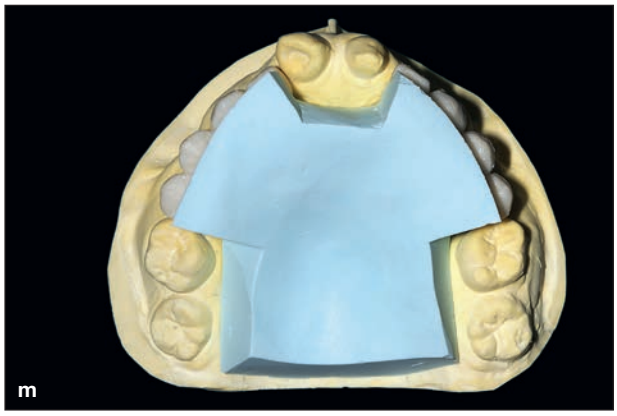

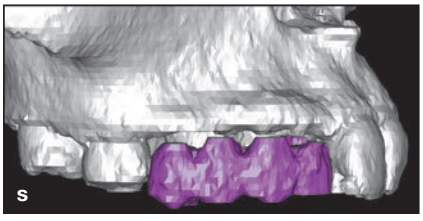

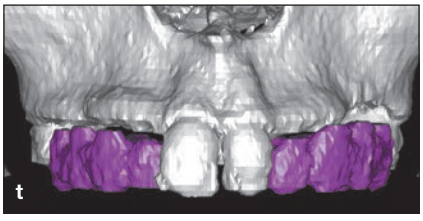

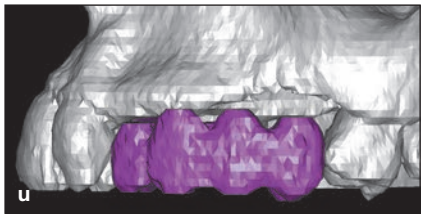

Fig 14-3 *cont.* / *(m to o)* After the wax-up positions are transferred to the working cast, the future implant positions are anticipated and transferred as well.[14–17] *(p to u)* The proportions are analyzed. The diagnostic template fabricated according to the orthodontic setup model conveys an idea of the ideal future shape of the alveolar ridge.

orthodontic proposal to the patient could be tested for plausibility and the anatomical conditions could be analyzed with cone beam computed tomography (CBCT) (Figs 14-3p to 14-3u).

Based on strategic considerations, the maxillary sites selected for implant placement were the canine and premolar sites (Figs 14-3v to 14-3aa; see Box 14-1). A strategically advantageous choice of implant positions is particularly important in cases that also necessitate orthodontic treatment. Orthodontic treatment began as soon as the implants were functioning. In the maxilla, the treatment procedure followed the IO sequence.

Fig 14-6 / *(a)* Silicone gingival prosthesis in the anterior maxilla. *(b)* Without the prosthesis, the vertical tissue loss in the region and gingival recessions at the canines become apparent. *(c and d)* Preoperative lateral views of the maxilla. *(e)* Panoramic radiograph of the preoperative situation.

After systematic periodontal treatment, distraction osteogenesis was performed for vertical ridge augmentation (Figs 14-6f to 14-6i; see chapter 9). After this, horizontal augmentation was additionally required and was performed by means of bone spreading and GBR (Figs 14-6j and 14-6k). Two implants were placed in the maxillary lateral incisor sites as abutments for a partial denture (Fig 14-6l). In the pontic area of the central incisors, the soft tissue was carefully conditioned with a provisional partial denture before the definitive superstructure was placed (Figs 14-6m to 14-6o).